DOI 10.1007/s11223-021-00344-5
Strength of Materials, Vol. 53, No. 5, September, 2021

A LINEAR ELASTIC FRACTURE MECHANICS ANALYSIS OF THE PRE-CRACKED CONCRETE FAILURE MECHANISM UNDER MODES I, II, III, AND IV LOADING CONDITIONS

J. Fu,[a] H. Haeri,[b,1] M. D. Yavari,[c] V. Sarfarazi,[d] M. F. Marji,[e] and M. Guo[a]

UDC 539.4

In this study, pre-cracked cubic specimens of concrete materials were especially prepared in a concrete laboratory to study the breaking process of brittle solids. Then, the linear elastic fracture mechanics concept of the stress intensity factor and the experimental methods were used to investigate the failure mechanism of pre-cracked concrete specimens under compression. The crack propagation mechanism and the ultimate strengths of these specimens were obtained in the laboratory. Several numerical analyses were also carried out on the pre-cracked specimens, using the finite element method and ABAQUS software package. The damage location and convergence diagram of the differential evolutionary algorithm under mode I, II, III or IV loading conditions were investigated for the cubic pre-cracked concrete specimens containing a single center crack with different inclination angles. The crack propagation mechanisms obtained numerically were compared with the corresponding experimental ones proving the proposed method's feasibility.

Keywords: convergence diagram, damage location, fracture mechanics, cubic pre-cracked concrete specimen.

Introduction. Numerous studies have been conducted on the identification of systems and the detection of damage in brittle materials by using a variety of methods developed for this purpose. Basically, the damage detection methods are divided into two general categories: the destructive and the non-destructive identification methods. The destructive methods using the structural sampling examine the extent of damage or even failure in the materials' specimens. Today, the non-destructive methods have become very popular due to their cost-effectiveness. The non-destructive methods are also divided into local and general. The local injury detection methods have some limitations, including the penetration depth of the waves and the location of the injury to conduct the test [1]. The destructive methods based on the linear elastic fracture mechanics have been used by many researchers to study the fracturing mechanism of the concrete and rock structures [2–4]. Benedetti et al. [5] proposed an approximate solution for the problem of a vibrating damaged RC beam with opening–closing (breathing) cracks. Methods based on examining vibration (dynamic) properties of a structure to detect and estimate the possible damage can be classified as methods based on the use of intensification frequency, shape of modes, frequency response function (FRF), and curvature of the modes, modal strain energy, dynamic softness, damping, Ritz vectors, time-frequency analyses, updating the finite element model, and wave propagation theory [6].

[a]School of Civil Engineering and Transportation, North China University of Water Resources and Electric Power, Zhengzhou, China. [b]State Key Laboratory for Deep GeoMechanics and Underground Engineering, Beijing, China ([1]haerihadi@gmail.com, h.haeri@bafgh-iau.ac.ir). [c]Department of Mining Engineering, Islamic Azad University, Bafgh Branch, Bafgh, Yazd, Iran. [d]Department of Mining Engineering, Hamedan University of Technology, Hamedan, Iran. [e]Department of Mine Exploitation Engineering, Faculty of Mining and metallurgy, Institute of Engineering, Yazd University, Yazd, Iran. Translated from Problemy Prochnosti, No. 5, pp. 98 – 110, September – October, 2021. Original article submitted January 19, 2021.

TABLE 1. Ingredient Ratios and Mechanical Properties of the Concrete Specimens

Ingredients ratio (%)			Mechanical properties				
PPC	Fine sand	Water	Tensile strength (MPa)	Uniaxial compression strength (MPa)	Fracture toughness ($MPa \cdot m^{1/2}$)	Modulus of elasticity (GPa)	Poisson's ratio
44.5	22.5	33.0	3.81	28.0	2.0	17.0	0.21

For example, several experimental and numerical studies have been devoted to explaining the fracture and damage mechanisms of rock and concrete structures [7–17]. In this study, the cracking mechanism of cubic specimens with single crack has been studied both experimentally and numerically. The damage location and convergence diagram of the differential evolutionary algorithm under mode I, II, III and IV of loading are investigated in the pre-cracked concrete cubic specimens (containing single crack in the central part of the specimen) with different inclination angles. The MATLAB and the ABAQUS software are used in this study to numerically simulate the breakage mechanism based on the concrete damaged plasticity (CDP) model. The crack propagation patterns obtained numerically are compared with the corresponding experimental results showing the validity of the accomplished numerical results.

1. Methodology. The crack propagation paths of the single-crack cubic specimens have been experimentally investigated. The same experimental specimens are numerically modeled by a versatile finite element code known as ABAQUS. It has been shown that the corresponding numerical results are in good agreement with their experimentally observed counterparts. In this research, it is attempted to study the breakage process of the pre-cracked cubic specimens of concrete. Therefore, the damage location and the convergence diagram of differential evolutionary algorithm under four modes I (opening mode), mode II (shearing mode), mode III (tearing mode), mode IV (in-plane axial mode or in-plane buckling mode) in the pre-cracked cubic specimens of concrete. In the experimental work, the fracture paths were studied for single-cracked cubic specimens with different inclination angles. In these samples, different damage types have been defined and all the results are presented in separate tables. Also, the parametric analysis and the optimization algorithm are presented by considering 3% noise during the analysis.

A proper mixture of Portland Pozzolana cement (PPC), fine sands and water are to produce the pre-cracked concrete specimens in the form of cubes with sides of 150 mm. Table 1 gives the mechanical properties of the prepared concrete specimens tested in the laboratory before inserting the cracks

2. Application of the Structural Response in the Time Domain to Identify the Damage. Time-domain responses of structures are dynamic responses that can be measured directly and at a lower cost compared to the other dynamic responses. To obtain the response over time, the structures must first be solved according to the principles of structural dynamics. If the total applied force to the structure is $F(t)$, the second-order differential equation with several degrees of freedom governing the dynamic behavior of structures can be written as [13]:

$$M\ddot{X}(t) + C\dot{X}(t) + KX(t) = F(t), \tag{1}$$

where M, C, and K are the matrices of mass, damping, and stiffness of the structure and $\ddot{X}(t)$, $\dot{X}(t)$, and $X(t)$ are the acceleration vectors, velocity, and displacement vectors of the structure at moment t, respectively. Numerical integration methods can be divided into two broad categories of explicit and implicit methods in which the most famous approaches are: (i) the central difference method; (ii) the Hubert method; (iii) the Wilson-theta method; (iv) the Newmark method.

The first method is basically an explicit method while the other three methods belong to the implicit methods. In general, the explicit conditional methods are stable, and if a sufficiently small step is not selected, the answers will diverge, while the implicit methods are unconditionally stable with proper selection of the relevant parameters. On the other hand, two types of errors are introduced in numerical integration, where, the first type of error is related to the amplitude decay and the second one is related to the period elongation of the system response.

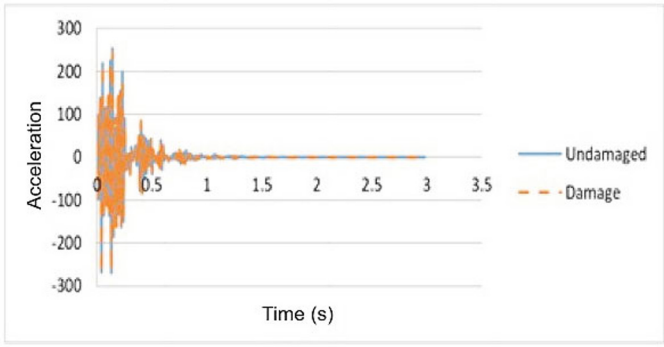

Fig. 1. Acceleration responses in the undamaged and damaged structures throughout the range of usage.

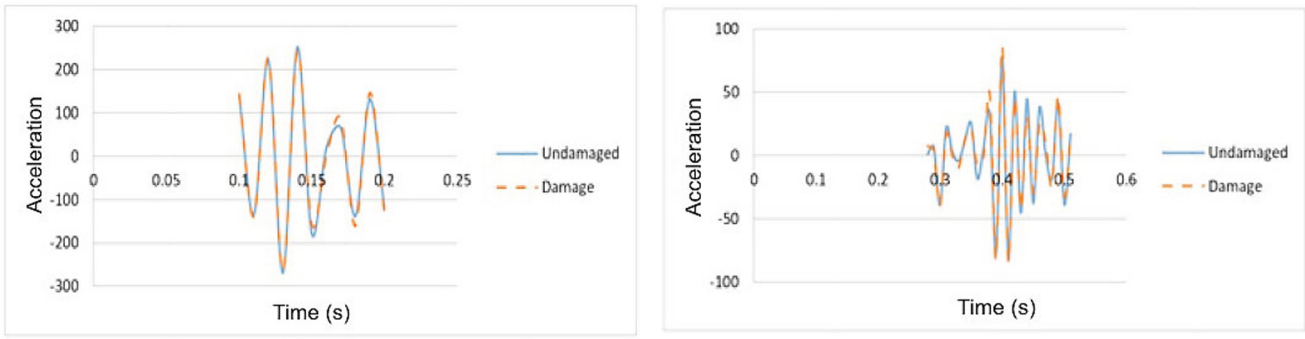

a b

Fig. 2. Acceleration responses in the undamaged and damaged structures in the range of (a) 0.1 to 0.2 and (b) 0.3 to 0.5.

In this respect, the Newmark method is more appropriate than the Wilson-theta and Hubert methods. In this method, the error related to the amplitude decay is insignificant and only the elongation period is considered. Therefore, the Newmark method is used to solve the desired equations [15].

Acceleration is a time-dependent function of a structure containing very comprehensive and useful information that can be used to identify the possible damage in the structure. It means that any damage occurrence will lead to changes in dynamic responses including acceleration of structures.

As it can be seen in Fig. 1, the accelerated response of the damaged structure compared to the undamaged structure has been changed.

To show the changes more clearly, the two intervals (0.2, 0.1) and (0.5, 0.3) were examined (Fig. 2).

2.1. Failure Identification of the Optimization Method. The purpose of this study is to identify the local damages of structures by the optimization method. The general form of the optimization problem related to fault identification can be expressed as follows:

$$\begin{aligned} &\text{Find: } X^T = \{x_1, x_2, \ldots, x_n\}, \\ &\text{Minimize: } w(X)\ (X^l \le x_i \le X^u) \end{aligned} \tag{2}$$

where X is the damage variable vector containing the location and severity of the unknown damages, X^l and X^u are, respectively, the lower and upper limits of the failure vector, and w is the objective function that must be minimized.

2.2. The Objective Function. The objective function can be considered as one of the most important parts of an optimization problem. The objective function is a measure by which the convergence value of the algorithm and the stop time of the algorithm execution are determined. It is up to the user to select the appropriate target function

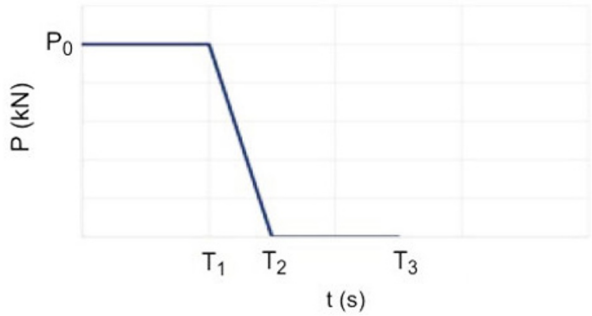

Fig. 3

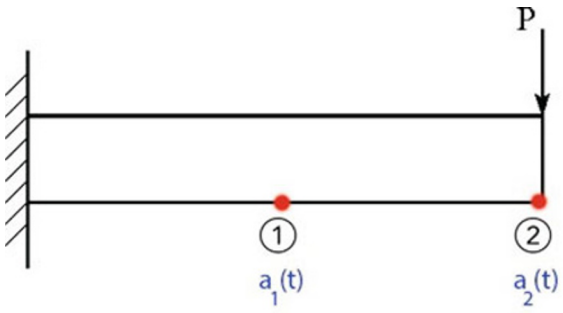

Fig. 4

Fig. 3. Load P (kN) entered into the structure versus the time t (s).
Fig. 4. The force applied and the acceleration obtained in a cantilever beam.

according to the specific circumstances of the damage identification issue. In this study, according to the multiple damage reliability criterion [4], the objective function was defined as follows:

$$w(X) = \frac{\left| a_d^T a(X) \right|}{(a_d^T a_d)(a(X)^T a(X))}, \tag{3}$$

where a_d is the acceleration vector of the damaged structure and $a(X)$ is the acceleration vector of the analytical model.

If acceleration was measured at more than one point in the structure, the accelerations obtained at different points were arranged as a series of columnar vectors.

2.3. Implementation Steps of the Proposed Damage Identification Method. The steps for detecting damage in structures using time range responses and metaphysical optimization method are performed as follows:

Step 1: Apply a single, impact load to the structure as shown in Fig. 3. Of course, in programming the computer codes, the program can receive any kind of the desired load.

Step 2: Analyze the damaged structure using the Newmark method and extract acceleration of the structure at the two desired points according to Fig. 4. For a cantilever beam, according to Eq. (1), the accelerations at points *1* and *2* are obtained.

Step 3: form the objective function consisting of the structural acceleration response in the damage state and the acceleration of the analytical model according to Eq. (3).

Step 4: Minimize the objective function formed in the previous step using the metaphysical optimization algorithm and determine the location and extent of damage.

3. Finite Element Analyses of the Structural Damage. The standard finite element code known as ABAQUS is used in this study to numerically simulate the inelastic behavior of concrete based on the concrete damaged plasticity (CDP) model. The tensile and compressive loading conditions in concrete may be modeled by considering the isotropic damaged elasticity concept [18]. Table 2 lists the CDP parameters used in the finite element method (ABAQUS).

The geometries of the centered cracks with different inclination angles in the cubic concrete specimens are illustrated in Fig. 5.

In the experimental work, the uniaxial compression loading was conducted on cubic specimens of concrete materials (containing a single crack in the central part of the specimen) with different inclination angles. Such specimens prepared from PCC, fine sands, and water were tested in a compressive testing apparatus in a concrete mechanics laboratory.

The fracture patterns of these four cases including the tensile cracks initiated from the crack tips and propagated in the applied load direction are shown in Fig. 6.

TABLE 2. The Concrete Material Definition in Finite Element Analyses

Parameter	Value
Dilation angle	56°
Eccentricity	0.1
The ratio of initial equibiaxial compressive yield stress to initial uniaxial compressive yield stress	1.16
The ratio of the second stress invariant on the tensile meridian	0.667
Viscosity parameter	0.0001

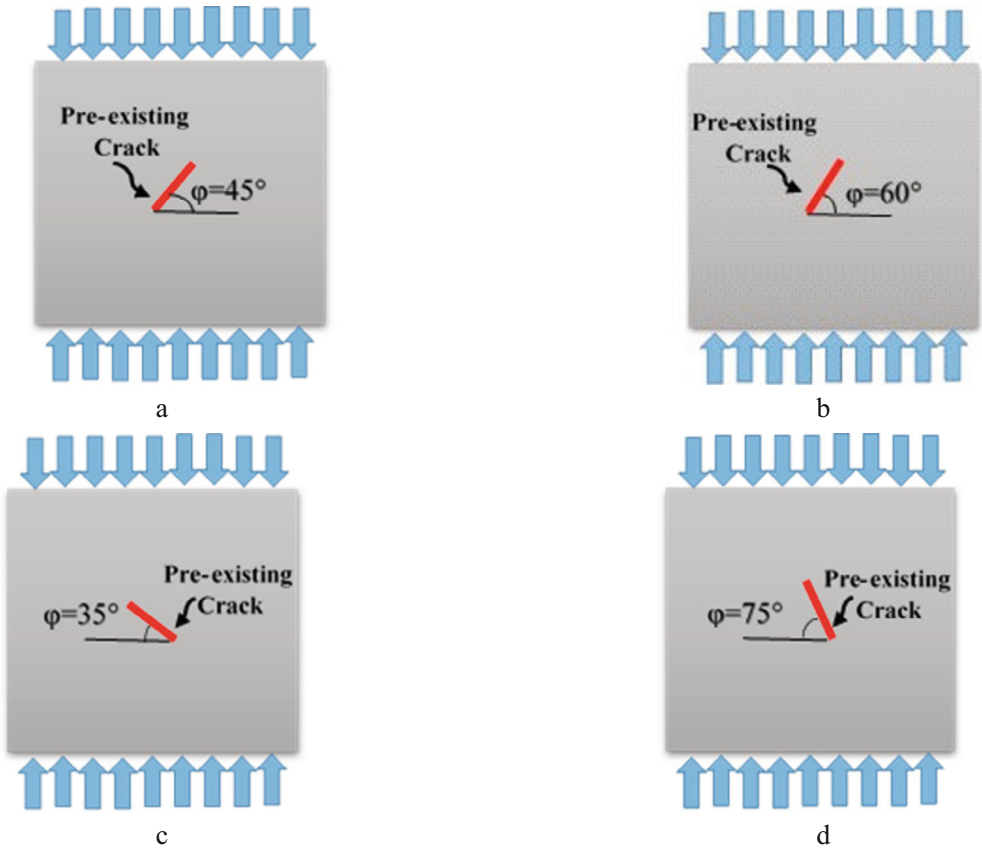

Fig. 5. The geometries of cubic specimens with a single centered inclined crack. Here and in Figs. 6 and 7: (a) $\varphi = 45°$; (b) $\varphi = 60°$; (c) $\varphi = 35°$; (d) $\varphi = 75°$.

Then, some of the experimental works were simulated numerically via the ABAQUS software. Crack propagation in the cubic concrete specimens with a single centered crack at different inclination angles were numerically modeled, and these results were compared with the corresponding experimental ones (Fig. 6).

Comparing the numerical results in Fig. 7a–d with the corresponding experimental results given in Fig. 6a–d, respectively, their close correlation was observed.

3.1. Cubic Specimens with a Single Centered Crack Inclined at 45°. Damage in elements of the pre-cracked cubic specimens was modeled via the elastic modulus reduction. Parameters required for the optimization are presented in Table 3.

To examine the accuracy of the proposed method, three different modes (modes I, II, and III) were investigated and presented in Table 4.

Considering a damping coefficient of 5%, the optimization continued until all iterations were reached $k_{\max} = 1000$ or the target function value did not change significantly after 100 iterations. The experimental and numerical failure patterns of cubic specimens with a single centered crack inclined at 45° are presented in Fig. 8.

TABLE 3. Parameters Required for Optimization

Parameter	Symbol	Value
Number of particles	NP	20
Mutation coefficient	F	0.60
Probability	CR	0.30
Maximum iterations	k_{max}	1000

TABLE 4. Different Modes of Loading Conditions for Considering Damage in Cubic Specimens with a Single Centered Cracks Inclined at 45°

Mode I		Mode II		Mode III	
No. of element	Damage intensity	No. of element	Damage intensity	No. of element	Damage intensity
8	0.30	4	0.30	4	0.30
–	–	12	0.30	8	0.30
–	–	–	–	12	0.20

a b c d

Fig. 6. The failure and fracture patterns of cubic concrete specimens with a single centered crack at different inclination angles.

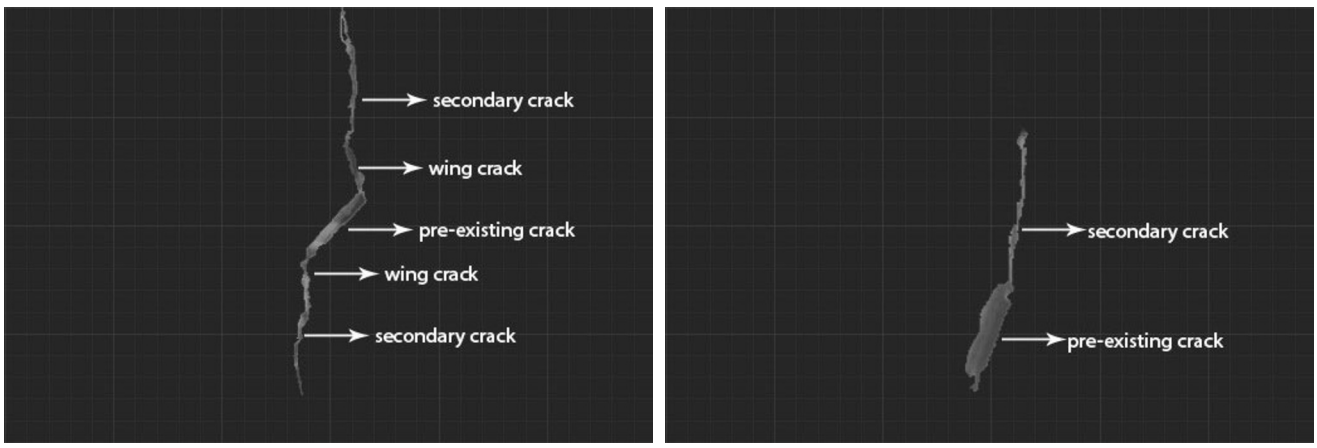

a b

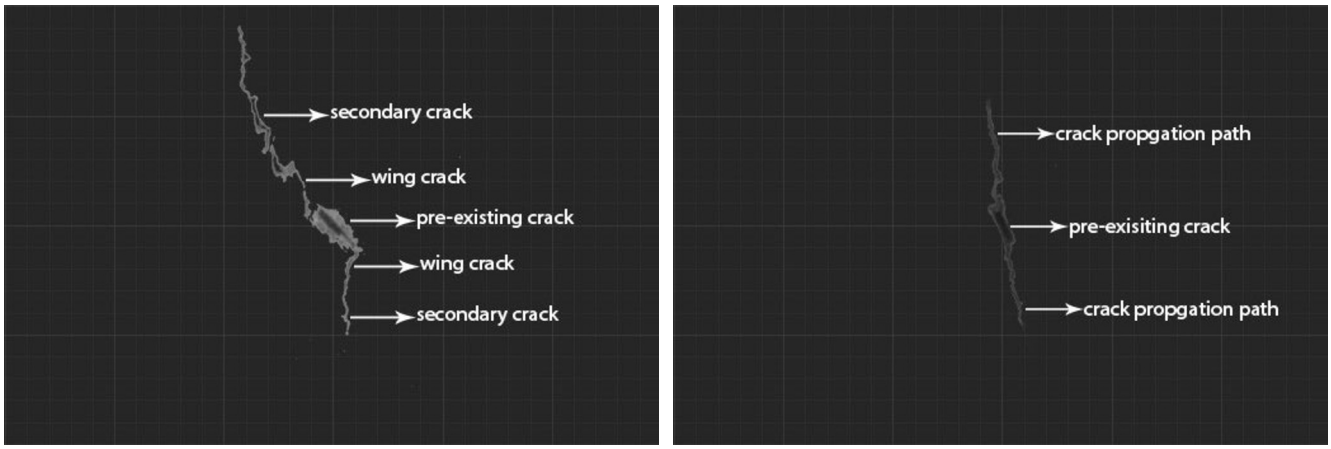

c d

Fig. 7. The numerically simulated cubic concrete specimens with a center crack oriented at different inclination angles.

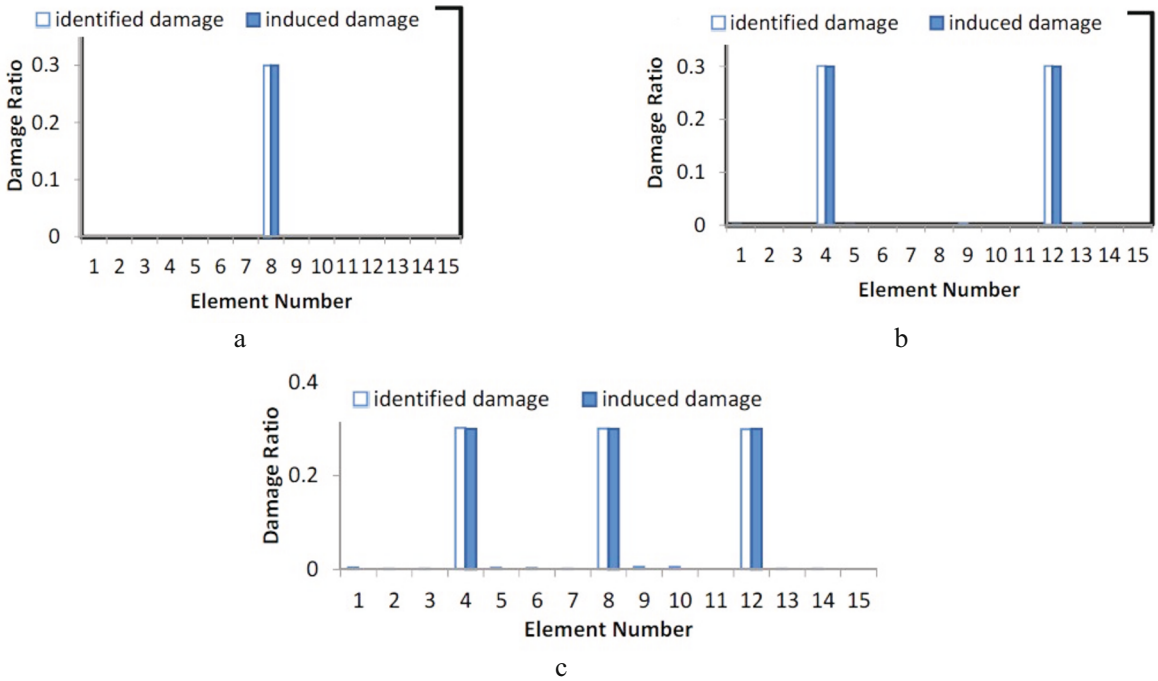

Fig. 8. Predicting damage location under mode I (a), II (b), and III (c) loading conditions in a cubic specimen with a single central crack inclinated at 45°.

Moreover, the convergence diagrams of the optimization algorithm for these three modes can also be predicted. Figure 9 depicts the diagrams of damage identification in a single-cracked specimen with a crack inclination angle of 45° under mode I, II, and III loading conditions.

As can be seen in Fig. 9, the proper damage locations and their intensities are detected by the proposed method with a high accuracy, regardless of the noises. These results confirm the high effectiveness of the proposed method for predicting the structural damage to the concrete specimens.

According to the convergence diagrams, it can be observed that with 300 iterations, the algorithm reaches convergence at the last 100 iterations and no significant changes can be seen at higher iterations.

3.2. Cubic Specimens with a Single Centered Crack Inclined at 60°. To examine the accuracy of the proposed method, four different modes of damage were investigated as presented in Table 5.

TABLE 5. Different Damage Modes Observed in Cubic Specimens with a Single Centered Crack Inclinated at 60°

Mode I		Mode II		Mode III		Mode IV	
No. of element	Damage intensity	No. of element	Damage intensity	No. of element	Damage intensity	No. of element	Damage intensity
12	0.20	12	0.20	12	0.20	15	0.20
–	–	13	0.30	13	0.30	16	0.15
–	–	–	–	14	0.30	17	0.20

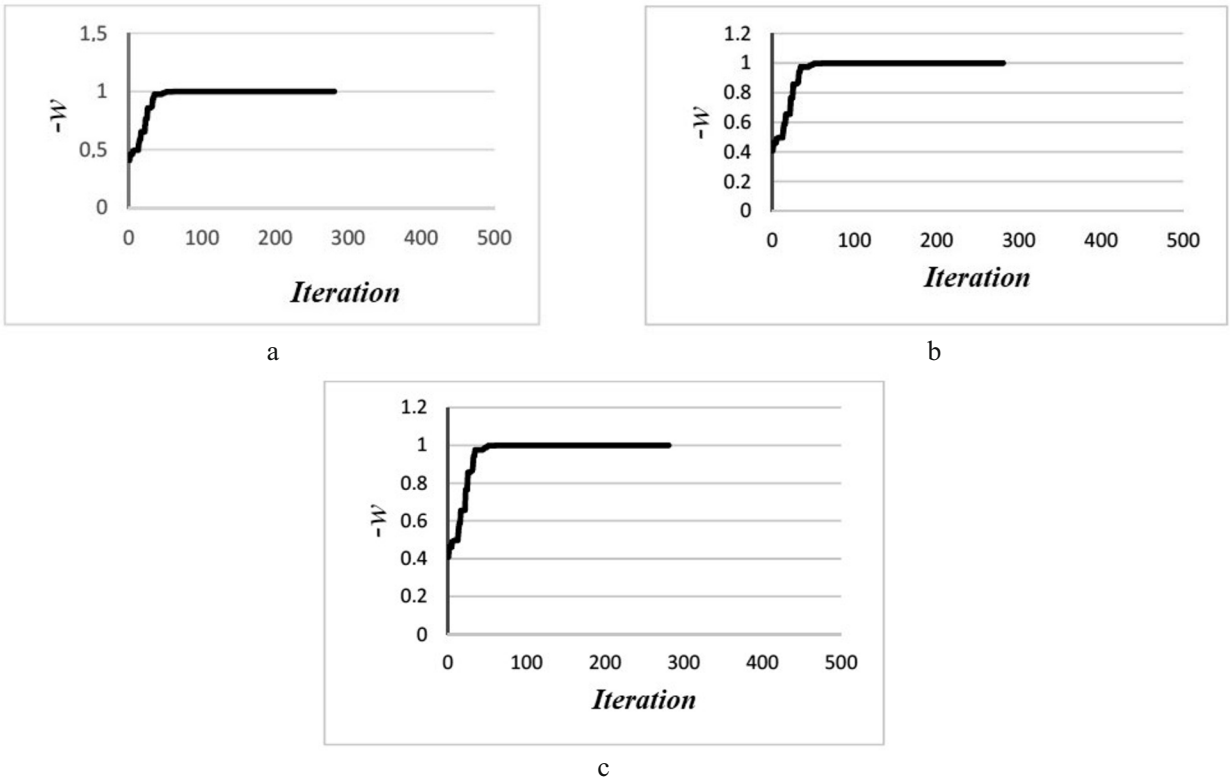

Fig. 9. Convergence diagram of differential evolutionary algorithm under mode I (a), mode II (b), and mode III (c) loading conditions in a single-cracked specimen with crack inclination angle of 45°.

Considering a damping coefficient of 5%, the optimization was continued until all iterations were reached $k_{\max} = 1000$ or the target function value did not change significantly after 100 iterations.

The damage detection diagrams for the cubic concrete specimens with a centered single crack inclined at 60° and considering I, II, III, and IV modes are shown in Fig. 10.

Moreover, Fig. 11a–d show the convergence diagrams of the optimization algorithm for the concrete specimens under these four loading modes.

According to Figs. 11, the proposed method detects the damage location and intensity with a high accuracy, regardless of the noise effect. These results confirm high effectiveness of the proposed method. Again, it can be observed that at 300 iterations, the algorithm reached convergence at the last 100 iterations with no significant change in the results.

3.3. Cubic Specimens with a Single Centered Crack Inclined at 35°. To examine the accuracy of the proposed method presented in this study, various modes of damage process are investigated and presented in Table 6. Results of each mode are presented with the simulation on MATLAB and ABAQUS softwares. In this mode,

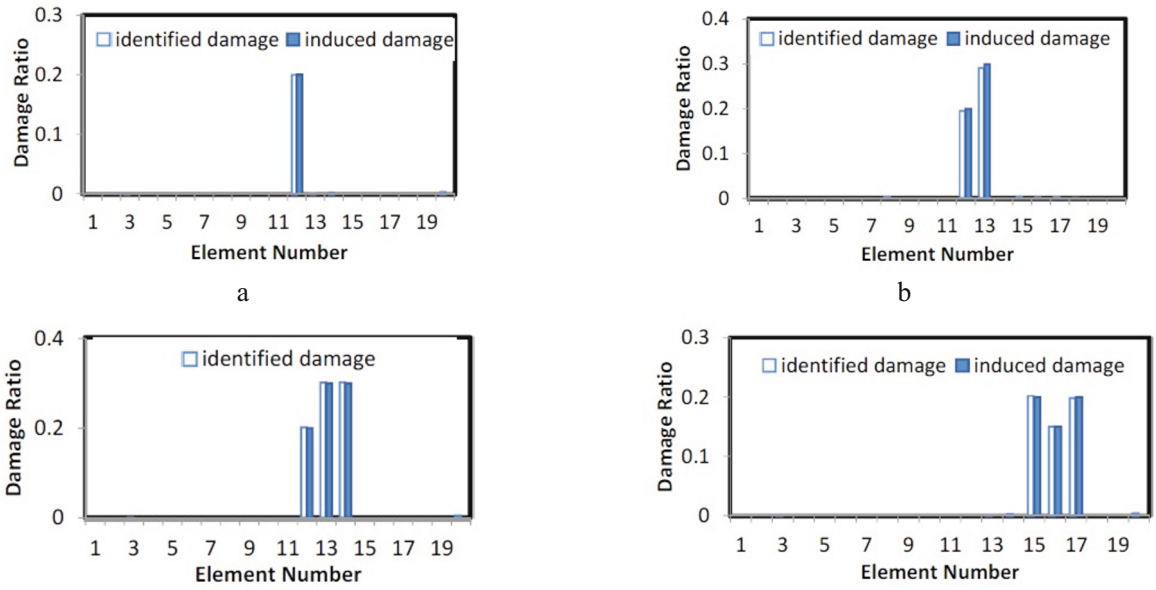

Fig. 10. Predicting damage location under loading modes of I (a), II (b), III (c), and IV (d) in cubic specimens with a single centered crack inclinated at 60°.

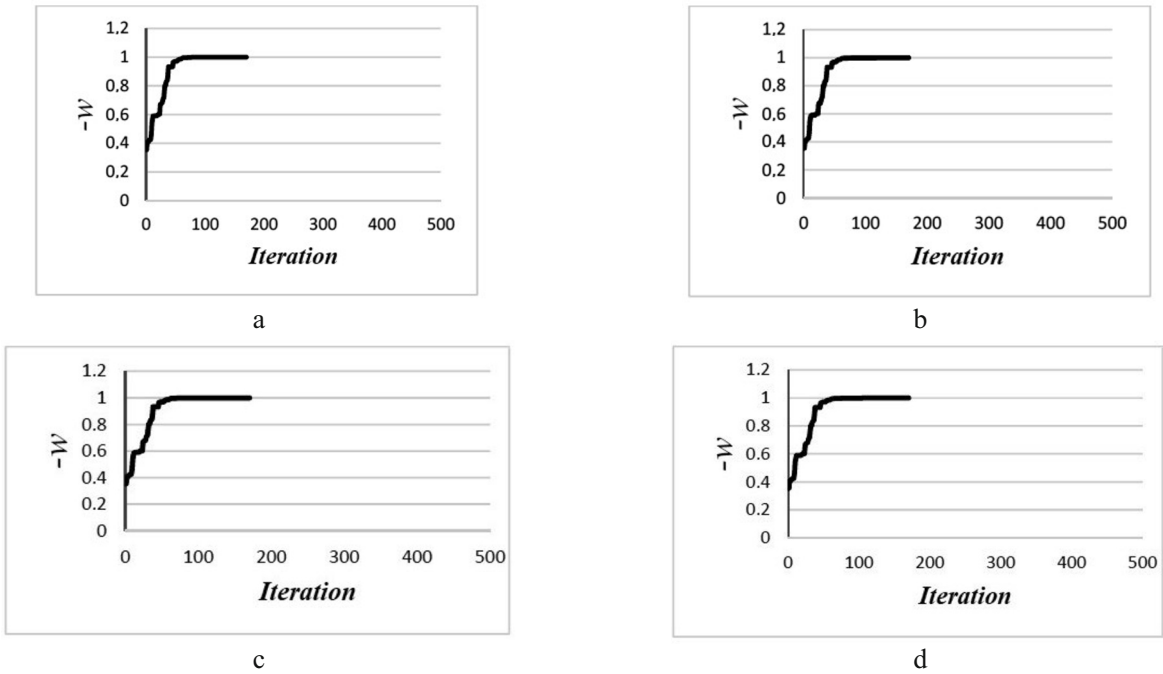

Fig. 11. Convergence diagrams for differential evolutionary algorithm in concrete specimens with centered single cracks inclined at 60° under loading modes I (a), II (b), III (c), and IV (d).

damping coefficient has been considered as 5% and optimization continues until total number of iterations reaches $k_{\max} = 3000$ or the value of target function does not change significantly after 500 iterations.

Damage identification diagrams in cubic specimens with crack inclination angle of 35° under the modes I, II, and III loading conditions are shown in Fig. 12. The optimization algorithm convergence diagrams of the specimens for these modes of loading are graphically presented in Fig. 13.

TABLE 6. Different Damage Intensities under Three Modes of Loading for Cubic Specimens with a Single Cenered Crack Inclined at 35°

Mode I		Mode II		Mode III	
No. of element	Damage intensity	No. of element	Damage intensity	No. of element	Damage intensity
3	0.10	16	0.10	3	0.10
–	–	–	–	16	0.10

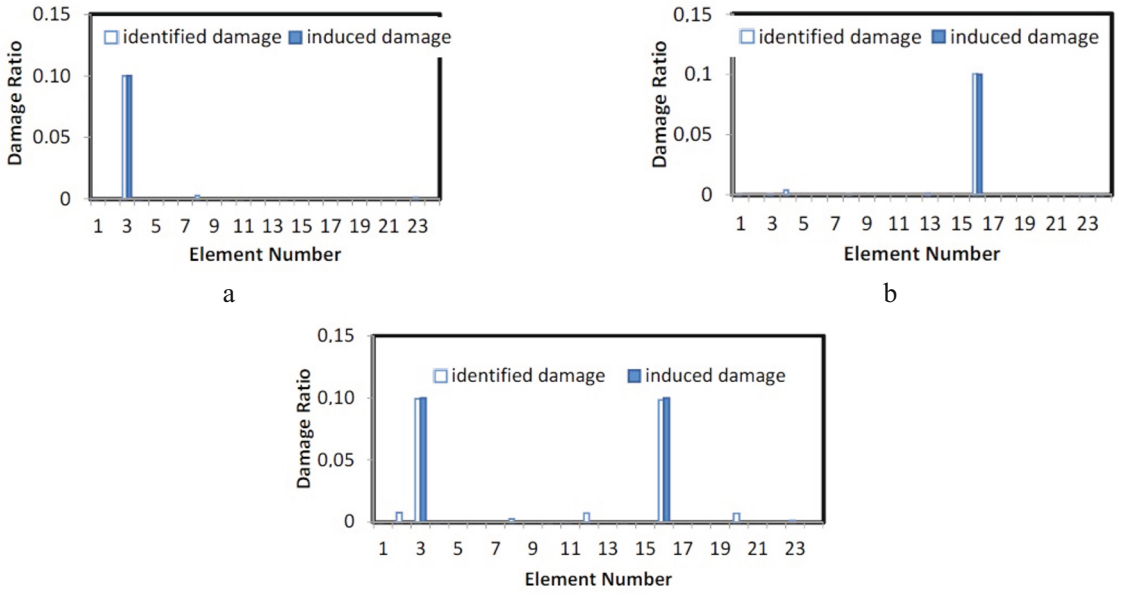

Fig. 12. Predicting damage location for concrete specimens under modes I (a), II (b), and III (c) loading conditions considering the centered single-cracked cubic specimens with crack inclination angle of 35°.

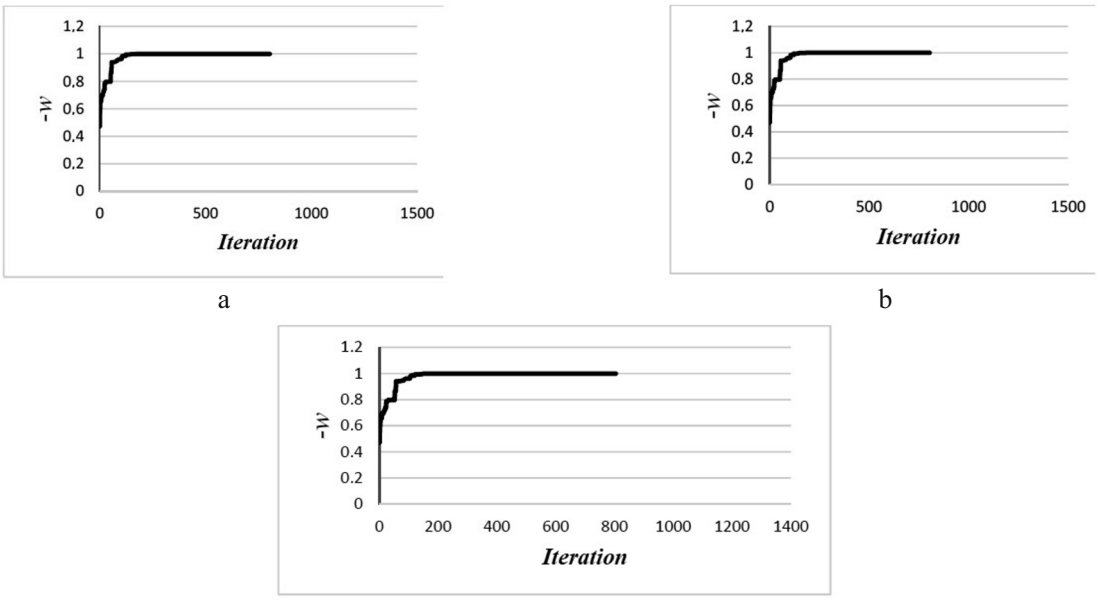

Fig. 13. Convergence diagrams of differential evolutionary algorithm for modes I (a), II (b), and III (c) loading conditions in the centered single-cracked cubic specimens with crack inclination angle of 35 °.

TABLE 7. The Three Modes of Loadings Considered for Damages in the Centered Single-Cracked Cubic Specimens with the Crack Inclination Angle of 75°

Mode I		Mode II		Mode III	
No. of element	Damage intensity	No. of element	Damage intensity	No. of element	Damage intensity
5	0.63	13	0.63	5	0.10
–	–	–	–	13	0.10

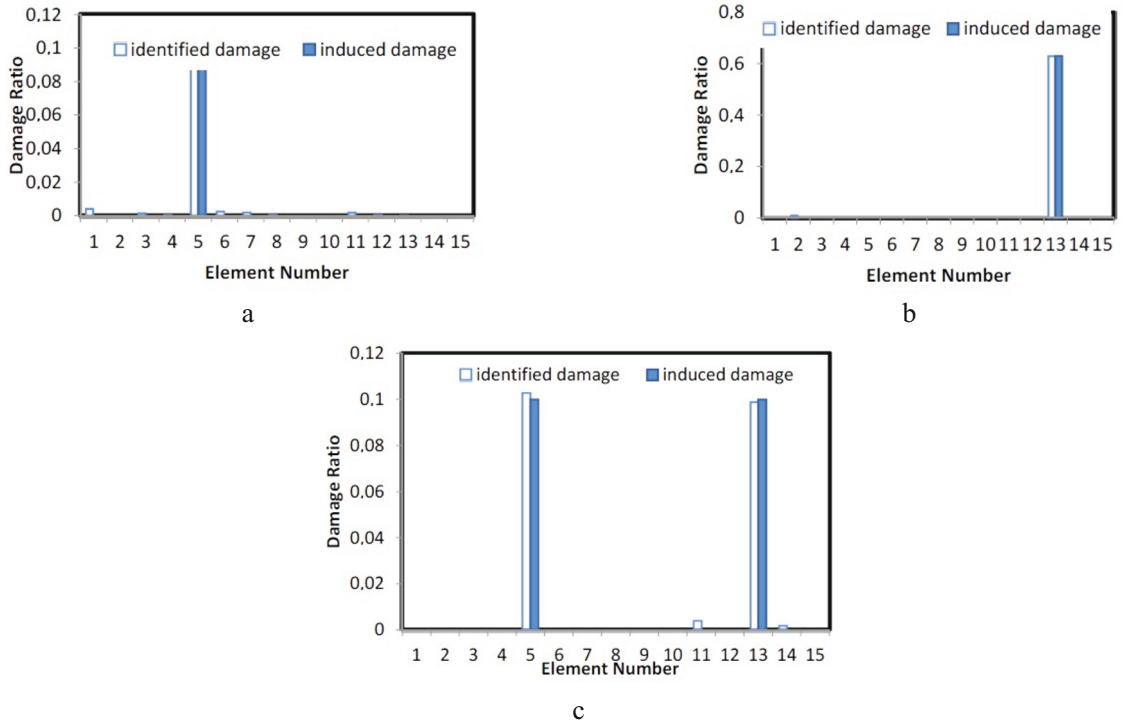

Fig. 14. Predicting damage locations for modes I (a), II (b), and III (c) of loading conditions in the centered single-cracked cubic specimens with a crack inclination angle of 75°.

As shown in Fig. 13, the proposed method can accurately identify the damage intensity regardless of noise effects. It can also be observed that with 800 iterations, the function reached convergence at the last 500 iterations.

3.4. Cubic Specimens with a Single Centered Crack Inclined at 75°. To examine the accuracy of the results, three damage modes were considered as presented in Table 7. In these damage modes, the damping coefficient was preset at 5%, and the optimization process continued until the total number of iterations reached $k_{\max} = 1000$ or the target function value did not change significantly after 200 iterations.

Figure 14 illustrates the damage identification diagrams for cubic specimens with a center crack inclination angle of 75° under the loading modes of I, II, and III. Figure 15 depicts their corresponding optimization algorithms for the convergence diagrams. According to the results shown in these figures, the proposed method properly identified the damages' location and intensity with a high accuracy, regardless of the noise effects.

Conclusions. In this study, the damage location and convergence diagram of the differential evolutionary algorithm under modes I, II, III or IV of loading conditions in the cubic pre-cracked concrete specimens containing a single centered crack with different inclination angles were investigated. The MATLAB and ABAQUS software were used to numerically simulate the breakage mechanism based on the concrete damaged plasticity (CDP) model. The crack propagation mechanisms obtained numerically were compared with the corresponding experimental results showing the validity of the numerical analyses. The damage acceleration in a concrete specimen was used as a

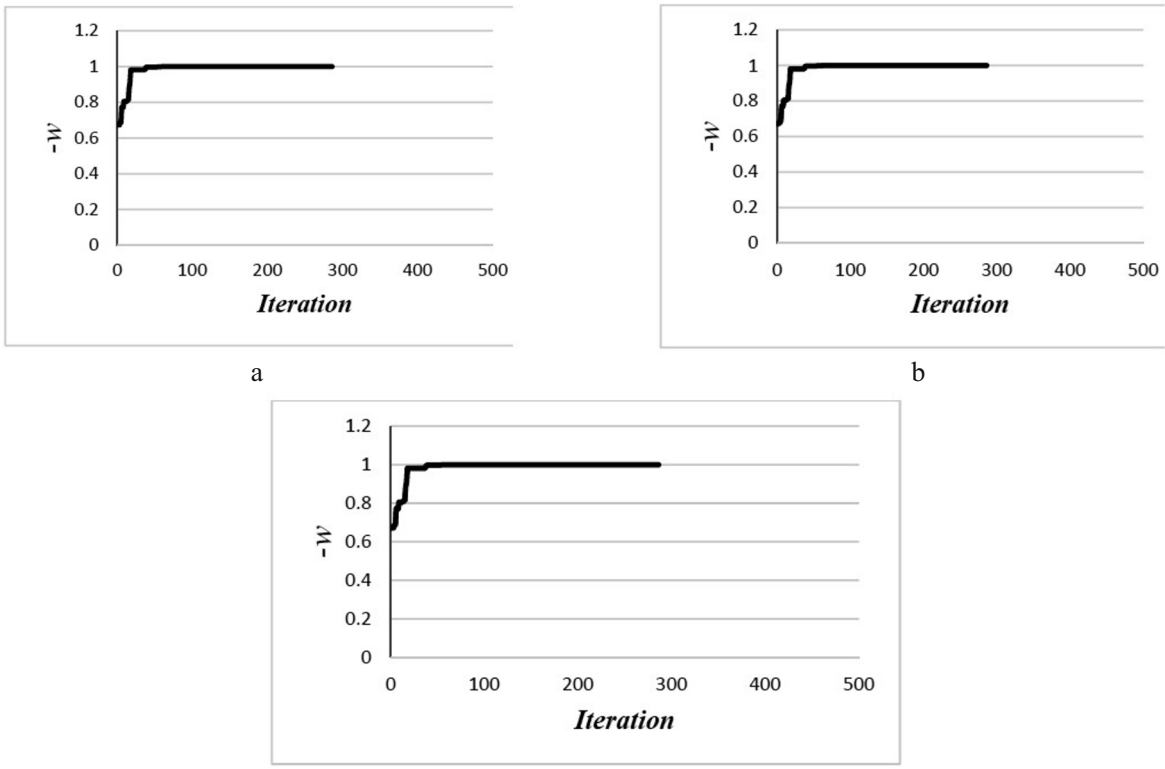

Fig. 15. The convergence diagrams of differential evolutionary algorithm for modes I (a), II (b), and III (c) loading conditions in the centered-single cracked cubic specimens with crack inclination angle of 75°.

criterion for detecting the structural damages. To calculate the acceleration, the Newmark method was used. At first, the damage detection problems were reduced to optimization problems, which were then solved using the differential evolutionary algorithm. In order to examine the effectiveness of the proposed method and the damage detection process, the modeling was carried out with the reduction of the elastic modulus of the elements. The results showed a high effectiveness of the proposed method in identifying the location and intensity of the damages in concrete specimens.

Acknowledgments. This work was financially supported by National Natural Science Foundation of China (Grant No. 51608117), Key Specialized Research and Development Breakthrough Program in Henan province (Grant No. 192102210051).

REFERENCES

1. T. Vo-Duy, V. Ho-Huu, H. Dang-Trung, et al., "Damage detection in laminated composite plates using modal strain energy and improved differential evolution algorithm," *Procedia Engineer.*, **142**, 182–189 (2016).
2. Z. H. Ding, M. Huang, and Z. R. Lu, "Structural damage detection using artificial bee colony algorithm with hybrid search strategy," *Swarm Evol. Comput.*, **28**, 1–13 (2016).
3. A. Kaveh, S. R. Hoseini Vaez, and P. Hosseini, "Enhanced vibrating particles system algorithm for damage identification of truss structures," *Sci. Iran.*, **26**, No. 1, 246–256 (2019).
4. G. F. Gomes, Y. A. D. Mendéz, S. S. da Cunha, and A. C. Ancelotti, "A numerical–experimental study for structural damage detection in CFRP plates using remote vibration measurements," *J. Civil Struct. Health Monit.*, **8**, No. 1, 33–47 (2018).

5. A. Benedetti, G. Pignagnoli, and M. Tarozzi, "Damage identification of cracked reinforced concrete beams through frequency shift," *Mater. Struct*., **51**, 147 (2018), https://doi.org/10.1617/s11527-018-1275-z.
6. D. Dinh-Cong, T. Vo-Duy, V. Ho-Huu, et al., "An efficient multi-stage optimization approach for damage detection in plate structures," *Adv. Eng. Softw*., **112**, 76–87 (2017).
7. M. F. Marji, H. Hosseini-Nasab, and A. H. Kohsary, "A new cubic element formulation of the displacement discontinuity method using three special crack tip elements for crack analysis," *JP J. Solids Struct*., **1**, No. 1, 61–91 (2007).
8. M. Fontan, A. Ndiaye, D. Breysse, et al., "Soil–structure interaction: Parameters identification using particle swarm optimization," *Comput. Struct.*, **89**, Nos. 17–18, 1602–1614 (2011).
9. H. Haeri and M. F. Marji, "Simulating the crack propagation and cracks coalescence underneath TBM disc cutters," *Arab. J. Geosci.*, **9**, No. 2, 124 (2016).
10. O. Abdeljaber, S. Avci, M. Kiranyaz, et al., "Real-time vibration-based structural damage detection using one-dimensional convolutional neural networks," *J. Sound Vib*., **388**, 154–170 (2017).
11. V. Sarfarazi, H. Haeri, M. F. Marji, and Z. Zhu, "Fracture mechanism of Brazilian discs with multiple parallel notches using PFC2D," *Period. Polytech.-Civ*., **61**, No. 4, 653–663 (2017).
12. S. R. H. Vaez and N. Fallah, "Damage identification of a 2D frame structure using two-stage approach," *J. Mech. Sci. Technol.*, **32**, No. 3, 1125–1133 (2018).
13. K. Samir, B. Brahim, R. Capozucca, and M. A. Wahab, "Damage detection in CFRP composite beams based on vibration analysis using proper orthogonal decomposition method with radial basis functions and cuckoo search algorithm," *Compos. Struct.*, **187**, 344–353 (2018).
14. D. Dinh-Cong, S. Pham-Duy, and T. Nguyen-Thoi, "Damage detection of 2D frame structures using incomplete measurements by optimization procedure and model reduction," *J. Adv. Eng. Comput*., **2**, No. 3, 164–173 (2018).
15. D. Dinh-Cong, H. Dang-Trung, and T. Nguyen-Thoi, "An efficient approach for optimal sensor placement and damage identification in laminated composite structures," *Adv. Eng. Softw.*, **119**, 48–59 (2018).
16. S. Bureerat and N. Pholdee, "Adaptive sine cosine algorithm integrated with differential evolution for structural damage detection," in: Proc. of the 17th Int. Conf. on Computational Science and Its Applications, Springer, Cham (2017), pp. 71–86.
17. N. Fallah, S. R. H. Vaez, and A. Mohammadzadeh, "Multi-damage identification of large-scale truss structures using a two-step approach," *J. Build. Eng.*, **19**, 494–505 (2018).
18. H. D. Hibbitt, B. I. Karlsson, and E. P. Sorensen, *ABAQUS User's Manual*, Dassault Systèmes Simulia Corp., Providence, RI (2012).